Fluid Flow and Heat Transfer of Natural Convection around Heated Vertical Cylinders*
(Effect of Cylinder Diameter)

Fumiyoshi KIMURA**, Tatsuo TACHIBANA**, Kenzo KITAMURA***
and Tsutomu HOSOKAWA**

Natural convective flows of water induced around heated vertical cylinders have been investigated experimentally. Special interests were paid to the influences of cylinder diameter on the turbulent transition and also on the local heat transfer characteristics of the cylinders. The diameters of the cylinders were varied systematically from 10 to 165 mm. Visualizations of the flows around the cylinder and of the surface temperatures of the heated cylinders have been carried out to determine the onset of turbulent transition. The result showed that the onset of turbulent transition shifts toward downstream with decreasing the cylinder diameters, when, in particular, the diameters are smaller than 60 mm. Moreover, the local heat transfer coefficients of the cylinder show marked increase in the both regions of laminar and turbulent flows with decreasing the diameters.

Key Words: Natural Convection, Heat Transfer, Vertical Cylinders, Size Effect, Power Equipment

1. Introduction

Natural convective flows around heated vertical cylinders appear in a wide variety of power equipment and environmental situations. Therefore, intensive studies have been carried out to investigate their flow and heat-transfer characteristics. However, most of the previous studies have dealt with the natural convections over large cylinders, where their diameters are larger than the boundary layer thickness, and, thus, a boundary layer assumption may hold. Meanwhile, very few works have dealt with the natural convections around small cylinders or thin wires, where the boundary layer assumption no longer holds.

To the best of the authors' knowledge, we can only cite the analytical works by Fujii and Uehara[1] and by Isahai and co-workers[2] for the latter studies. Fujii and Uehara[1] have adopted a perturbation method to a laminar boundary layer flow over small cylinders, and have proposed a correlation equation for the local Nusselt numbers, while Isahai and co-workers have carried out the numerical analysis on the flow and temperature fields around the cylinder of finite length and diameter. They have calculated two-dimensional, full-elliptic equations of momentum and heat transport using the finite difference method. Based on the numerical results, they have also proposed a correlation equation for the laminar heat transfer.

Although the analytical results mentioned in the above will be helpful for the estimation of heat transfer rates, the results have not been confirmed by the experiments. Besides, very little information is available at present, in particular, on the turbulent transition of flow over small cylinders or wires. The turbulent heat transfer from small cylinders is another problem that has not been clarified yet. The previous analyses have predicted that the heat transfer by a laminar natural convection is enhanced significantly with decreasing the cylinder diameter, while it is still uncertain whether the turbulent heat transfer from the small cylinders or wires is enhanced or not compared with that from the large cylinders or wide plates.

Taking account of the above, the present authors have

* Received 30th July, 2003 (No. 03-4167)
** Department of Mechanical and System Engineering, Himeji Institute of Technology, 2167 Shosha, Himeji, Hyogo 671–2201, Japan.
E-mail: kimura@mech.eng.himeji-tech.ac.jp
*** Department of Mechanical Engineering, Toyohashi University of Technology, Tempaku-cho, Toyohashi, Aichi 441–8580, Japan

carried out the experimental investigations on the flow and heat transfer of natural convection over small cylinders. The experiments begin with the visualization of flow to obtain detailed information on the natural convective flows induced around the small cylinders. The surface temperatures of the test cylinders were, next, visualized with liquid-crystal thermometry. The visualization was intended to investigate the onset of turbulent transition over small cylinders and also to obtain comprehensive information on the heat transfer, in particular, by the transitional and turbulent flows. Moreover, referring to those visual observations, the local heat transfer coefficients of the test cylinders were measured quantitatively by using thermocouples. Based on these measurements, the influences of cylinder diameters on the flow and heat transfer around the small cylinders were discussed.

2. Experimental Apparatus and Measurements

A schematic illustration of the present experimental apparatus is given in Fig. 1. The apparatus consist of a cylinder and a stage that sustains the cylinder. The diameter of the test cylinder, D, was varied as D = 10, 15, 26, 38, 60, 89 and 165 mm. The length of the cylinder was kept constant at 1 200 mm, which is long enough to realize a fully turbulent flow over the cylinder. The test cylinders were fabricated with a vinyl chloride or acrylic resin, hollow tube, and stainless-steel-foil heaters 30 μm thick. The heaters were glued on the outer surface of the tube and connected in series. A foam-styrene thermal insulation was stuffed into the tube to inhibit a conduction heat loss from the heater to the inside of the tube. A constant-surface-heat-flux condition was accomplished over the cylinder by supplying AC power to the heaters.

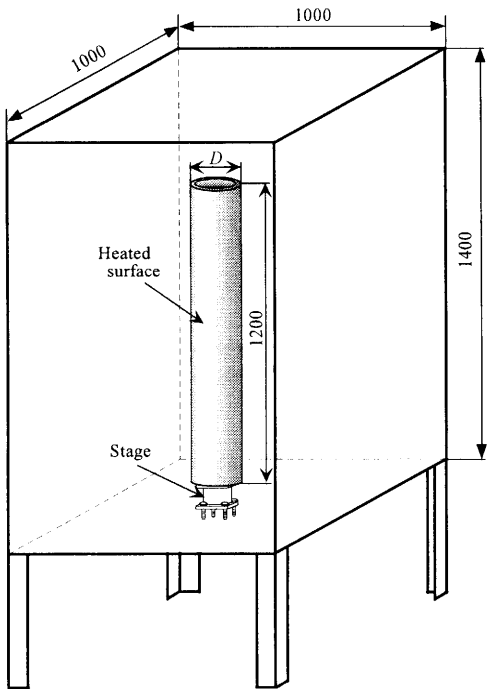

Fig. 1 Experimental apparatus

For the sake of the heat transfer measurement, Chromel-Alumel thermocouples of 100 μm diameter were spot-welded on the back of the heaters in the axial direction of the test cylinders. These thermocouples measure local surface temperatures, T_{wx}, in the stream-wise direction. The temperature of the ambient fluid, T_∞, was also measured with the thermocouples, which were placed 50 mm apart from the lower edge of the test cylinder and in the same horizontal plane. From the preliminary measurements, the conduction heat loss from the heaters to the inside of the test cylinder was estimated as less than 5% of the total heat generation of the heaters. The loss was negligibly small, so that the surface heat flux, q_w, was calculated by $q_w = Q/A$, where Q and A stand for the electrical power input to the heater and the total surface area of the heaters, respectively. Then, by using the heat flux, q_w, and the temperature difference between the surface and the ambient temperatures, T_{wx} and T_∞, the local heat transfer coefficients, h_x, were defined as:

$$h_x = q_w/(T_{wx} - T_\infty) \tag{1}$$

Taking account of the relative easiness of the heat transfer measurements and also of the visualizations, water at room temperature was utilized as a test fluid. The above apparatus was placed on the floor of the rectangular water tank. The tank of 1 000 mm × 1 000 mm cross-sectional area and 1 400 mm deep was utilized in the experiment. Thermo-physical properties of non-dimensional parameters mentioned in the following chapters were estimated at the film temperatures, $T_f = (T_w - T_\infty)/2$. The maximum modified Rayleigh numbers based on the length of the cylinder, Ra_L^* (= $g\beta q_w L^4/\lambda\nu\alpha$), has reached to $Ra_L^* = 1.4 \times 10^{14}$, in the present experiments. The number is considered high enough to attain a fully turbulent flow over the cylinder.

3. Results and Discussions

3.1 Visualization of flow fields

In order to obtain comprehensive information on the turbulent transition over vertical cylinders, we have first carried out the flow visualization experiments using dye. The representative results are shown in Fig. 2 for the cylinders of various diameters, where uranine dissolved with water was utilized as a dye tracer. The dye was issued slowly from a long slit flush-mounted on the leading edge of the cylinders. The photos were taken from the side of the cylinders and their originals are color.

As is obvious from Fig. 2, the dye issued from the slit first flows along the cylinder surface, and then, gradually become unstable and generates lateral waves at a certain distance from the leading edge. The waves, then, sepa-

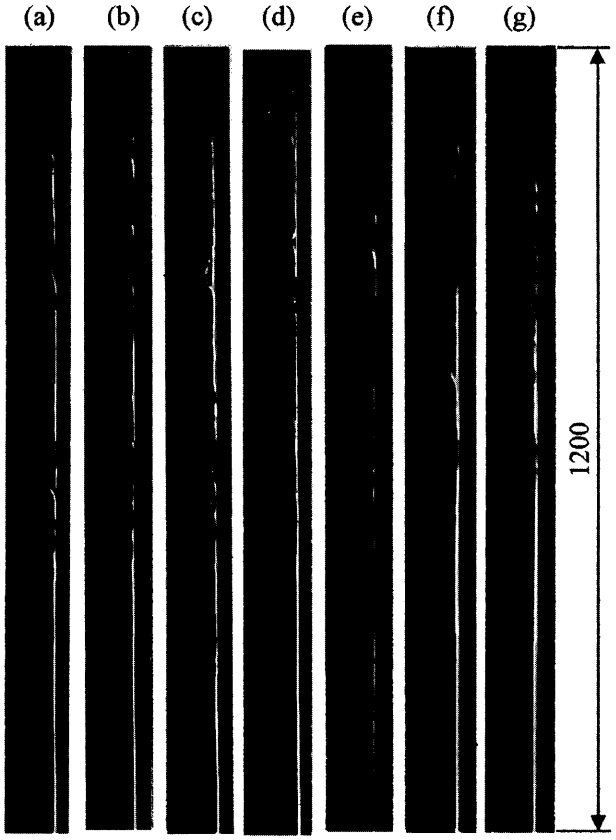

Fig. 2 Visualized flow fields. (a) $D = 165$ mm, (b) $D = 89$ mm, (c) $D = 60$ mm, (d) $D = 38$ mm, (e) $D = 26$ mm, (f) $D = 15$ mm, (g) $D = 10$ mm

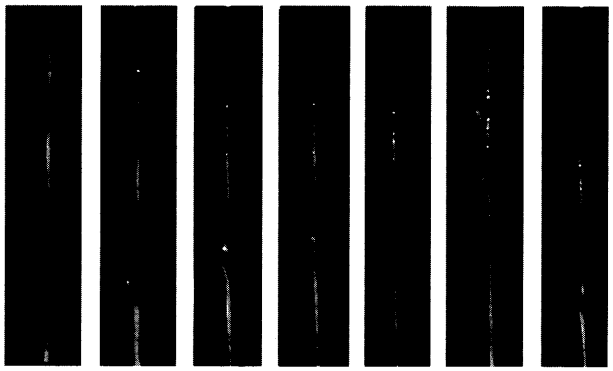

Fig. 3 Continuous pictures of separation ($D = 26$ mm)

rate from the surface and, finally, become distorted at certain places downstream from the separation. The figures also depict that the onset of separation shifts toward downstream with decreasing the cylinder diameter, in particular, when the diameters are less than 60 mm.

Figure 3 represents the continuous pictures of the flow separation over the cylinder of $D = 26$ mm. The figure demonstrates that the vortex, the axis of which is parallel to the peripheral direction of the cylinder, first appears upstream of the cylinder, and the vortex gradually becomes distorted toward downstream by involving the

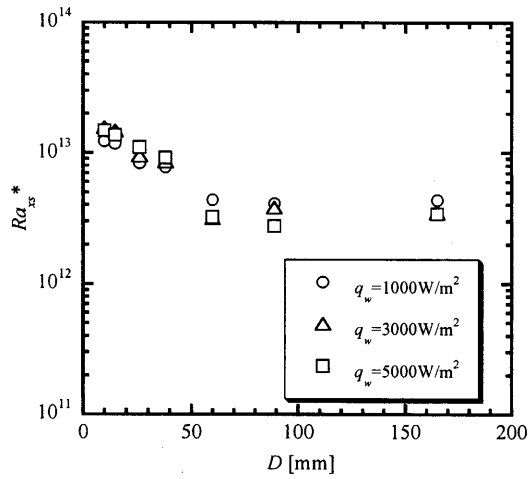

Fig. 4 Separation point

ambient fluid, and, finally, a fully turbulent flow is realized over the cylinder.

3.2 Onset points of turbulent transition

Next we'll discuss the onset of the turbulent transition over the cylinders. Based on the previous results of the flow visualizations, the turbulent transition begins with the separation of flow, so that we define the onset of the turbulent transition as the first beginning of the flow separation from the cylinder. According to the present observations, the separation points move irregularly with time. Thus, we define the separation points with their time-averaged location. In order to determine the location precisely, continuous pictures were first taken with a video camera, and, next, their still pictures were reproduced at a constant time-interval. Then, these measurements were repeated tens of times to obtain the average separation points.

The results thus obtained are given in Fig. 4. In the figure, the average distances from the leading edge to the separation points, x_s, are normalized with the modified Rayleigh numbers; Ra_{xs}^* $(= g\beta q_w x_s^4/\lambda\nu\alpha)$, and they are plotted in term of the cylinder diameters, D. The figure depicts that the critical Rayleigh numbers, Ra_{xs}^*, corresponding to the separation points gradually decrease with the diameter, while the numbers become identical for the cylinders with diameter larger than 60 mm. It is also obvious that the surface heat fluxes of the cylinder exert no serious influence on the critical Rayleigh numbers within the range of the present experiments.

3.3 Visualization of surface temperatures

In order to obtain comprehensive information not only on the temperature fields over the cylinders but also on the local heat transfer characteristics of the cylinders, the surface temperatures of the test cylinders were next visualized by means of liquid crystal thermometry. Figure 5 shows the typical examples of the visualized surface temperatures of the heated cylinders with various diameters. The photos in Fig. 5 were taken from the direction normal

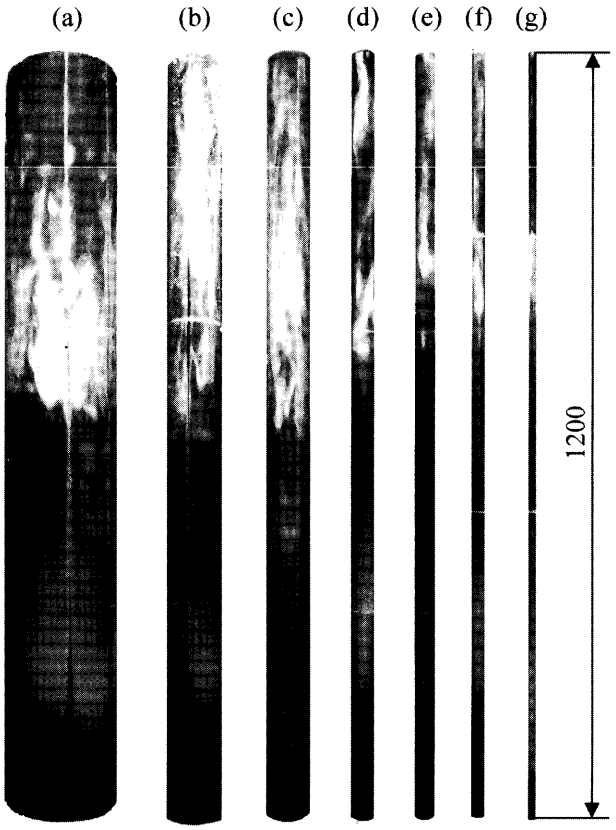

Fig. 5 Visualized surface temperatures. (a) $D = 165$ mm, (b) $D = 89$ mm, (c) $D = 60$ mm, (d) $D = 38$ mm, (e) $D = 26$ mm, (f) $D = 15$ mm, (g) $D = 10$ mm

to the cylinder. The liquid crystal utilized here changes its color from dark red, yellow, green to blue with increasing temperature. The colors dark red, yellow and green, and blue are reproduced as black, gray, and dark gray in the black and white photos of Fig. 5, respectively. These photos also represent the distributions of the local heat transfer coefficients, because the test cylinders were heated with a uniform heat flux and the temperature of the ambient fluid was kept constant. Thus, the black regions in the photos refer to the regions of low-temperature, high-heat-transfer, while the dark-gray regions represent the high-temperature, low-heat-transfer regions.

Taking these into account, we next discuss the results of Fig. 5. The surface temperatures near the bottom of the largest cylinder of $D = 165$ mm show a uniform temperature distribution circumferentially, while they increase gradually toward downstream. Although it is hardly visible in the small photos of Fig. 5 (a), a horse-shoe-shaped, low-temperature pattern first appears near the middle of the cylinder, and then, full-irregular, low-temperature patterns become visible at certain distance downstream from the horse-shoe-patterns. Similar temperature patterns are also apparent over the cylinders of $D = 89$ and 60 mm. The present author has carried out similar visualization experiments on the natural convection over vertical, flat

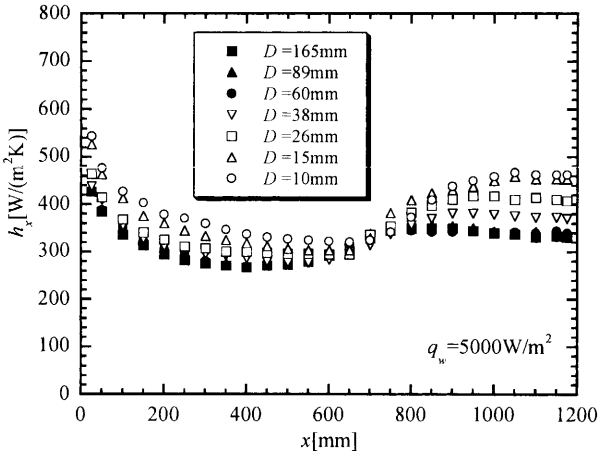

Fig. 6 Local heat transfer coefficients

plates[3),(4)], and have reported that the similar temperature patterns as above appear over the plate. Taking this into account, it seems that the turbulent transition over large cylinders undergoes the identical process as that over the flat plate. Meanwhile, it is worthwhile noting from Fig. 5 that the onset of the irregular temperature patterns gradually shifts toward downstream with decreasing the cylinder diameter, in particular, when the diameter becomes smaller than 60 mm.

Comparing the above results on the surface temperatures with those of the flow visualization, the following relationships were found: (1) The region of circumferentially uniform temperatures correspond to the laminar flow region, where the dye flows along the cylinder surface, (2) The region of the horse-shoe-shaped temperature pattern appears just downstream from the flow separation, thus, the region can be referred to as the transition region, (3) The region of the irregular temperature patterns corresponds to the fully turbulent region.

3.4 Local heat transfer characteristics

Based on the above visual observations, it was found that the onset of turbulent transition depends strongly on the cylinder diameter. Such change in the flow fields will also exert significant influences on the heat transfer from the cylinders. Thus, we subsequently carried out the measurements of the local heat transfer coefficients using thermocouples. One of the representative results is shown in Fig. 6 with the case of $q_w = 5000$ W/m^2, where the local heat transfer coefficients, h_x, defined by Eq. (1) are plotted with the stream-wise distance x from the leading edge.

Figure 6 reveals that the local heat transfer coefficients show the highest value at the leading edge. They decrease gradually with x, reach to a minimum value at some distance downstream, and then, they turn to increase, and show almost constant values. It is also obvious that the distributions are almost identical for the cylinders with diameters larger than 60 mm. On the other hand, the heat

transfer coefficients of the smaller cylinders depend on the cylinder diameter, and the higher coefficients are realized for the smaller cylinders. The location of the minimum coefficients also moves downstream with decreasing the diameter. The comparisons of these results with the flow visualizations revealed that the region from the leading edge to the minimum points of the coefficients correspond to the laminar flow region. Thus, the laminar heat transfer will be enhanced markedly by using small cylinders. The same is also true for the heat transfer by the transitional and turbulent flows. As is obvious from Fig. 6, the heat transfer coefficients downstream from the minimum points show monotonous increase with decreasing the diameters. The result demonstrates that the heat transfer is enhanced in the transitional and turbulent regions as well as in the laminar region over small cylinders.

In order to compare the present heat transfer data with the existing heat transfer correlations, all of the present data were re-plotted in the plane of the local Nusselt number, $Nu_x(=h_x \cdot x/\lambda)$, and the local modified Rayleigh number, Ra_x^*. The result is represented in Fig. 7. As is obvious from Fig. 7, the local Nusselt numbers of the large cylinders with $D \geq 60$ mm coincide fairly well with the previous laminar and turbulent correlations for the vertical flat plates proposed by Fujii[5], and by Vliet and Liu[6] and Authors[3], respectively. On the other hand, the local Nusselt numbers of the cylinders less than 60 mm show higher values than those estimated from the above correlations for both the laminar and turbulent flows.

As for the laminar heat transfer from the small cylinders heated with constant heat flux, Fujii and Uehara[1] have proposed a correlation equation by solving perturbation equations for the momentum and energy transport and the result was given as:

$$\frac{(Nu_x)_c}{(Nu_x)_p} = 1 + 0.370\left[\frac{x/r_0}{(Nu_x)_p}\right]^{\frac{5}{6}}, \quad \frac{x/r_0}{(Nu_x)_p} \leq 10^3 \quad (2)$$

Where, $(Nu_x)_c$ and $(Nu_x)_p$ are the local Nusselt numbers at the stream-wise location x for a cylinder and a flat plate, respectively, and r_0 stands for the radius of the cylinder. Meanwhile, Isahai et al.[2] have solved the two-dimensional, full-elliptic equations for the momentum and heat transport numerically, and have proposed a similar correlation equation as the above. The equation is expressed as:

$$\frac{(Nu_x)_c}{(Nu_x)_p} = 1 + 0.324\left[\frac{x/r_0}{(Nu_x)_p}\right]^{0.89}, \quad \frac{x/r_0}{(Nu_x)_p} \leq 1 \quad (3)$$

The present laminar Nusselt numbers were, next, compared with the above Eqs. (2) and (3). The representative result is shown in Fig. 8 with the case of $D = 10$ mm, where the local Nusselt numbers, $(Nu_x)_c$, are plotted in terms of the local Modified Rayleigh numbers, Ra_x^*. Figure 8 shows that the present laminar data agree fairly well with the Eqs. (2) and (3). The results were consistent for the other cylinders with different diameters. These results will also support the previous analyses.

Meanwhile, as was shown in Fig. 8, the local Nusselt numbers deviate from the above laminar values with further increase in the local Rayleigh numbers, Ra_x^*. The onset of the deviation will give a critical Rayleigh number for the turbulent transition. Based on this idea, we have measured the critical Rayleigh numbers, Ra_{xc}^* for the cylinders with various diameters. The results are as follows: $Ra_{xc}^* = 1.5\times10^{13}$ for $D = 10$ mm, $Ra_{xc}^* = 1.4\times10^{13}$ for $D = 15$ mm, $Ra_{xc}^* = 1.0\times10^{13}$ for $D = 26$ mm, $Ra_{xc}^* = 9\times10^{12}$ for $D = 38$ mm, and $Ra_{xc}^* = 4.5\times10^{12}$ for $D = 60$, 89 and 165 mm. We will find that these values correspond well with those for the onset of flow separation shown in Fig. 4.

With further increase in the Rayleigh numbers, the flow over the cylinders becomes fully turbulent. Figure 7 shows that the local Nusselt numbers of the turbulent flows

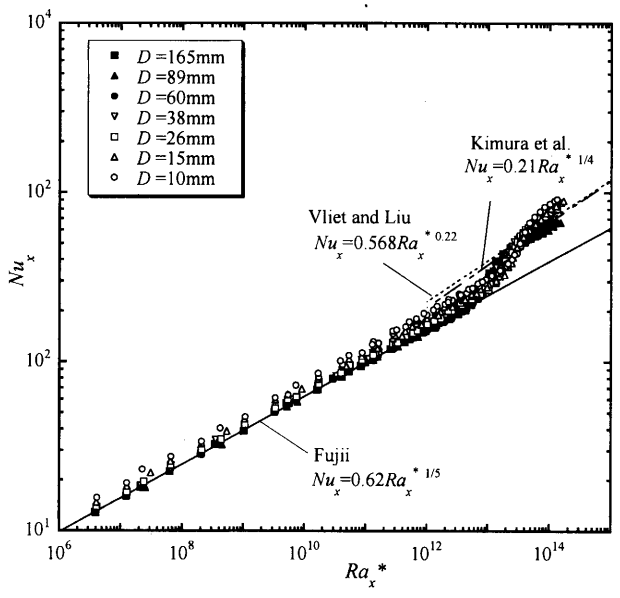

Fig. 7 Comparison of local Nusselt numbers

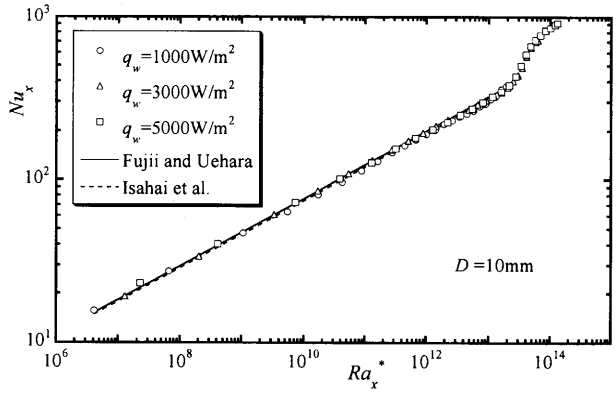

Fig. 8 Comparison of laminar Nusselt numbers

depend on the cylinder diameter, and that the smaller the cylinder, the higher the numbers that are attained. The result is note-worthy, because no one has reported such dependency of the cylinder diameters on the turbulent heat transfer. We have, therefore, tried to obtain a general correlation for the turbulent heat transfer, but the attempt failed. This is mainly due to the lack of the heat transfer data, in particular, in the region of the higher Rayleigh numbers. We are planning to conduct further experiments on high Rayleigh number flows in the near future.

4. Conclusions

The experimental investigations have been carried out on the fluid flow and heat transfer of natural convection induced around the vertical cylinders with various diameters. Special concerns were paid to the effect of cylinder diameter on the turbulent transition and also on the local heat transfer characteristics. The following results were obtained from the present experiments.

(1) The flow visualizations with dye showed that the turbulent transition over cylinders occurs through the following process. First, a lateral wave appears in the laminar-boundary-layer over the cylinder. Second, the wave gradually becomes unstable and a separation of flow happens at a certain distance from the leading edge. The flow, then, becomes distorted downstream and, finally, a full turbulent state is accomplished. The surface temperature visualizations with the liquid crystal thermometry also revealed that horse-shoe-shaped, low-temperature patterns first appear over the surface, and, then, the patterns change to an irregular pattern abruptly at some distance downstream.

(2) Based on these observations, the onset points of the turbulent transition were defined as the points of the flow separation, and they were measured with the cylinders of various diameters. The results showed that the critical Rayleigh numbers corresponding to the onset of the turbulent transition depend strongly on the cylinder diameters, and that the smaller the cylinders, the higher the numbers that are attained. However, the numbers are consistent for the cylinders with diameters larger than 60 mm.

(3) The stream-wise variations of the local heat transfer coefficients from cylinders were also measured with the thermocouples. The results showed that the minimum coefficients appear at the location just upstream from the flow separation, and also that the minimum points shift toward downstream with decreasing the cylinder diameter. The result shows that the turbulent transition is delayed markedly over the small cylinders. Moreover, the heat transfer coefficients of the small cylinders show higher values than those of the large cylinders as well as of the flat plates. Such increase in the coefficients is consistent in both regions of laminar and turbulent.

The present results will afford basic information on the turbulent transition of natural convection over cylinders with arbitrary diameters, but also will become a basis for the future analysis.

References

(1) Fujii, T. and Uehara, T., Int. J. Heat Mass Transf., Vol.13 (1970), pp.607–615.

(2) Isahai, Y., Suetsugu, K. and Hattori, N., Trans. Jpn. Soc. Mech. Eng., (in Japanese), Vol.67, No.653 (2001), pp.300–303.

(3) Kitamura, K., Koike, M., Fukuoka, I. and Saito, T., Int. J. Heat Mass Transf., Vol.28, No.4 (1985), pp.837–850.

(4) Kimura, F., Kitamura, K., Yamaguchi, M. and Asami, T., Trans. Jpn. Soc. Mech. Eng., (in Japanese), Vol.66, No.645 (2000), pp.1453–1461.

(5) Fujii, T., Advances in Heat Transfer, (in Japanese), Vol.3, (1976), pp.26–68, Yokendo.

(6) Vliet, G.C. and Liu, K.C., Trans. ASME, J. Heat Transf., Vol.91, No.4 (1969), pp.517–531.